physics

MDPI

Article

On the Difference between the Radii of Gluons and Quarks

Luis Augusto Trevisan [1,*], Carlos Mirez [2] and Djalma Inacio da Silva [3]

[1] Department of Mathemathics and Statistics, State University of Ponta Grossa (UEPG), Av. Carlos Cavalcante 4748, Ponta Grossa CEP 84031-990, Brazil
[2] Institute of Science, Engineering and Technology, Federal University of the Jequitinhonha and Mucuri Valleys (UFVJM), Rua do Cruzeiro 01, Teófilo Otoni CEP 39803-371, Brazil; carlos.mirez@ufvjm.edu.br
[3] Youdigital Solucoes E Sistemas LTDA, Rua Joao Gbur, 861, Terreo, Curitiba CEP 82640-000, Brazil; autocadrocks@gmail.com
* Correspondence: luisaugustotrevisan@uepg.br

Abstract: In this paper, in the scope of a non-extensive statistical model for the nucleon's structure function, the volume of the gluons in the nucleons and the relations among the temperature, T, the parameter "q" of Tsallis statistics, and the scattering energies, Q^2, are studied. A system of equations with the usual sum rules are solved for the valence quarks, the experimental results for the polarized structure function, and the estimated carried moments for gluons and quarks. Each state of T and q leads to a set of chemical potentials and different radii for gluons and quarks. We conclude that gluons must occupy a larger volume than the quarks to fit the fraction of the total momentum. A linear function of the temperature with Q^2 is obtained as an approach. The obtained range of temperatures is different from the previous models.

Keywords: gluonic halo; nucleon structure function; non-extensive statistical model

Citation: Trevisan, L.A.; Mirez, C.; da Silva, D.I. On the Difference between the Radii of of Gluons and Quarks. *Physics* **2021**, *3*, 1155–1166. https://doi.org/10.3390/physics3040073

Received: 7 March 2021
Accepted: 12 August 2021
Published: 25 November 2021

1. Introduction

An important issue in Quantum Chromodynamics (QCD) is how much momentum gluons carry in nucleons. Some authors suppose that gluons carry out almost half of the momentum in the nucleons [1,2], while others say this must be about 30% [3]. The theoretical predictions also have variations, between near 50% and 20% [4,5]. On this subject, many models were proposed to describe the structure function of the nucleon, among them, the statistical models.

The statistical models were in vogue in the late 1980s and early 1990s [6–20]. They basically describe the nucleon as a gas of fermions, confined in the MIT bag [21,22]. Despite the good agreement of such models with some features, the momentum sum is not well described by considering only statistical arguments. The corrections in those models were made by perturbative methods [9] or finite size corrections (FSC) [20].

In [23,24], the variables were fitted the variables by a system of equations with the usual sum rules for valence quarks, and the violation of the Gottfried sum rule (GSR) (see, e.g., [25]) is an additional result. The GSR violation may be used as information to fit the temperature. Another sum rule is the sum of moments of all particles, quarks, and gluons, which to be 1.

In [23,24] Trevisan and Mirez considered the effects of non-extensivity by Tsallis [26,27] to study the nucleon structure function. Three main variables—the temperature T, the q of Tsallis, and the radius R—were considered in these studies. The model proposed in [23,24] was an adaptation of the model by Bhalerao [20,28] to the non-extensivity. The q-exponential replaces the usual exponential in the distributions.

The non-extensivity describes some situations in which the sum of the entropies of two independent subsystems A and B with individual probability densities, $f^{(A)}$ and $f^{(B)}$, respectively, implying an additional term that depends on a variable q, and not a sum of the two entropies. In the limit $q \to 1$ the additivity (extensivity) is recovered. That is, the

entropy of the joint system is different from the sum of the entropy of subsystems but with some interaction.

Let us denote the $S_q[f^{\mathrm{A}}]$ and $S_q[f^{\mathrm{B}}]$ entropy of the A and B system, respectively; then:

$$S_q[f^{(\mathrm{A}+\mathrm{B})}] = S_q[f^{\mathrm{A}}] + S_q[f^{\mathrm{B}}] + (1-q)S_q[f^{\mathrm{A}}]S_q[f^{\mathrm{B}}]. \quad (1)$$

The exact form of the function $f^{(\mathrm{A})}$ ($f^{(\mathrm{B})}$, etc.) to be discussed in Section 2.

The use of Tsallis statistics is justified by considering the valon model [29,30]. The valon is considered to consist of the valence quark, sea quarks, and gluons around. This subsystem, with some entropy, interacts with another valon. Therefore, the sum of the entropies reflects this fact. Each cloud of quarks and gluons around the valence quarks overlaps with the neighbors so that the particles are indistinguishable (in sense that one cannot tell to which valence quark the particles belong to). In addition, the radius of each valence quark with its sea is considered the radius of the nucleon.

Recently, Deppman [31] gave a theoretical justification to use the Tsallis distribution to study QCD, and Cardoso et al. [32] studied the thermodynamical variables in the MIT bag model considering the non-extensivity.

Here, a new study, in which the momenta of gluons and quarks are computed separately, obeying, of course, the sum rule. Therefore, new independent variables occur, the radii of quarks

The paper is organized as follows. In Section 2, the model of [23,24] is discussed and modified to consider the sum of momenta of quarks and gluons separately. Section 3 gives results and discusses those. Section 3 provides studies with fixed temperature (and variable q and radius), variable temperature (fixed q and radius), and variable radius (q and temperature are fixed). The conclusions and final remarks are given in Section 4.

2. Theory and Methods

In the present picture, the nucleon is considered a spherical bag with a radius R. Inside the bag, there is a gas of massless partons (quarks, antiquarks, gluons) in equilibrium at temperature T.

In the nucleon center of mass frame, each parton can charge a maximum of half of the total momentum. The other half is shared by the other partons. Thus, the mass (energy) that a parton can bring is at most half the mass of the nucleon. Therefore, $M = 939$ MeV is used in what follows. The main point of this study is to use a different radius for quarks and gluons. Besides this, consider that partons are point particles that form the gas inside the spherical bag with the radius of the nucleon.

Following Bhalearao [20], the infinite momentum frame (IMF) is considered to obtain the particle distribution functions (PDFs) for quarks and gluons. Below, two frames are considered, namely, the proton rest frame and IMF, both moving with velocity $-v(\simeq -1)$ along the common z axis.

The interest of this study lies in the limit when the Lorentz factor, $\gamma \equiv (1-v^2)^{-1/2} \to \infty$. The dependence of the particle number on the Bjorken variable, x, is [20,28]

$$\frac{dn_\alpha(x)}{dx} = \frac{M^2 x V}{2} \int_{Mx/2}^{M/2} \frac{g f_\alpha(E) dE}{2\pi^2}, \quad (2)$$

for each particle α. Here, g is the spin-color degeneracy factor—16 for the gluons (see, for instance, [33]), and 6 for the quarks (antiquarks)—of some flavor α, V is the nucleon volume, and $f_\alpha(E)$ is the energy probability distribution, which is given by

$$f_\alpha(E) = \frac{1}{[1+(q-1)\beta(E-\mu_\alpha)]^{1/(q-1)} \pm 1}, \quad (3)$$

for the case $(E-\mu_\alpha) > 0$, where μ_α is the chemical potential for each kind of quark, and

$$f_\alpha(E) = \frac{1}{[1+(1-q)\beta(E-\mu_\alpha)]^{1/(1-q)} \pm 1}, \tag{4}$$

for the case $(E-\mu_\alpha) \leq 0$. In these expressions, $\beta = 1/T$ (in units of Boltzmann constant, k_B), where T is the temperature, and (+1) stays for fermions and (-1) for bosons. The corresponding Fermi–Dirac and Bose–Einstein distributions are recovered with $q \to 1$, where q remains a free parameter in this model.

There are some studies about how to apply the non-extensivity to fermions and bosons, see e.g., [34] and references therein. Parvan and Batacharya developed [34] the fermions and bosons distributions of the transverse momentum using the grand-canonical ensemble. If one expands Equation (3) and compares it with Equation (56) (the thermodynamical distribution part) of [34], a close similarity of the present *ansatz* is observed with a more rigorous study. The only difference is focusing on the longitudinal momentum in the present study.

From Equation (2), one obtains particle distributions, $n_\alpha(x)$, and the total number of particles, n_α. Following [20,28], one gets the following set of equations and constraints:

$$n_{u\uparrow} + n_{u\downarrow} - n_{\bar{u}\uparrow} - n_{\bar{u}\downarrow} = 2, \tag{5}$$

$$n_{d\uparrow} + n_{d\downarrow} - n_{\bar{d}\uparrow} - n_{\bar{d}\downarrow} = 1, \tag{6}$$

$$n_{s\uparrow} + n_{s\downarrow} - n_{\bar{s}\uparrow} - n_{\bar{s}\downarrow} = 0, \tag{7}$$

$$n_{u\uparrow} - n_{u\downarrow} + n_{\bar{u}\uparrow} - n_{\bar{u}\downarrow} = \Delta u, \tag{8}$$

$$n_{d\uparrow} - n_{d\downarrow} + n_{\bar{d}\uparrow} - n_{\bar{d}\downarrow} = \Delta d, \tag{9}$$

$$n_{s\uparrow} - n_{s\downarrow} + n_{\bar{s}\uparrow} - n_{\bar{s}\downarrow} = \Delta s, \tag{10}$$

$$\sum_{\text{all partons}} (\text{momentum fraction}) = 1. \tag{11}$$

In these equations, $n_{u\uparrow}(n_{u\downarrow})$ means the number of *up* quarks, with positive (negative) spin; $n_{\bar{u}\uparrow}$ denotes up anti-quark with positive orientation; and similarly for other (down, d, strange, s) quarks. Δu is the difference between the sum of the up quark and up anti-quark with positive polarization and the negative polarization sum; and similarly for other cases.

The following relations among the chemical potentials are used to solve the system:

$$\mu_{\bar{\alpha}\downarrow} = -\mu_{\alpha\uparrow}, \tag{12}$$

and

$$\mu_{\bar{\alpha}\uparrow} = -\mu_{\alpha\downarrow}. \tag{13}$$

We use $\Delta u = 0.83 \pm 0.03$, $\Delta d = -0.43 \pm 0.03$, $\Delta s = -0.10 \pm 0.03$ for the proton and $\Delta u = -0.40 \pm 0.04$, $\Delta d = 0.86 \pm 0.04$, $\Delta s = -0.06 \pm 0.04$ for the neutron. Equations (5) and (6) interchange for the neutron. The experimental data can be obtained for E142 [35], E143 [36], E154 [37,38], SMC [39], and HERMES [40] Collaborations.

Besides, the main proposal of the present study is to calculate the radius of gluons and quarks separately; therefore, Equation (11), which still holds, splits into two equations:

$$\sum_{\text{all quarks}} (\text{momentum fraction}) = 0.716 \pm 0.068, \tag{14}$$

and

$$\sum_{\text{gluons}} (\text{momentum fraction}) = 0.284 \pm 0.068, \tag{15}$$

according to [3]. Of course, the values may vary according to the reference or the model. Equations (14) and (15) can be written as follows:

$$\int_0^1 n_{\text{all quarks}}(x)xdx = 0.716 \pm 0.068, \tag{16}$$

and

$$\int_0^1 n_{\text{all gluons}}(x)xdx = 0.284 \pm 0.068, \tag{17}$$

The results with different combinations for the variables T (temperature), R (nucleon radius), and q (the Tsallis parameter for non-extensivity) are given in Section 3 just below.

3. Results

In the present study, the quark and gluon radii are varied in order to obtain the appropriate momentum. Recent studies [3] show that the gluons carry about 30% of the momentum. This value is close to one obtained in previous studies [23,24]. As usual, the violation of the GSR is an additional condition to be achieved. The experimental data [25,41,42] provides with the values in the interval [0.09, 0.15]. Therefore, one can consider

$$0.09 < \int_0^1 \bar{d}(x) - \bar{u}(x)dx < 0.15 \tag{18}$$

Moreover, the following convention will be used:

$$\int_0^1 \bar{d}(x)dx = \bar{D}, \tag{19}$$

and

$$\int_0^1 \bar{u}(x)dx = \bar{U}. \tag{20}$$

3.1. The Model with Constant Temperature

Here, the variation of the radius with the q is studied for the case of two different temperatures. The momentum of quarks is about 72%. Once the temperature is set, the radius and q are varied. For these variations, many solutions may exist.

Figure 1 shows the dependence of the radius R on the non-extensivity factor q. The radius is seen to decrease with q almost linearly, and q is smaller than 1. This result means that with more gluon interactions, the system called valon (a valence quark with the corresponding quark-antiquark and gluon cloud) [29] interacts more with another valon, changing its internal entropy.

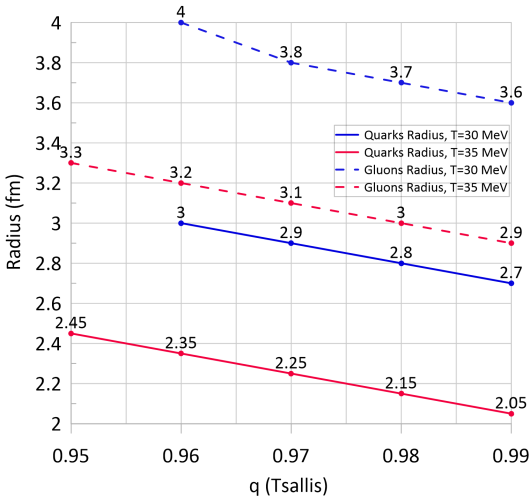

Figure 1. Variation of the radius, R, with the factor q of Tsallis statistics with two different temperatures, T. Dashed lines are for gluons, and straight lines are for quarks. Red lines are for $T = 35$ MeV and blue lines are for $T = 30$ MeV.

Each point in the quark's line of Figure 1 has five chemical potentials. Only those potentials are chosen which satisfy the sum of moments and violation of the GSR; see Table 1 for $T = 30$ MeV.

Table 1. The chemical potentials for the points of the blue continuous line of Figure 1. Each point is identified by the Tsallis non-extentivity parameter, q, and the radius, R. The sum of all quarks' momentum is about 0.72, and the valence quarks' momentum sum is about 0.48. The difference $\bar{D} - \bar{U}$ is around 0.14.

q	R (fm)	$\mu_{u\uparrow}$ (MeV)	$\mu_{u\downarrow}$ (MeV)	$\mu_{d\uparrow}$ (MeV)	$\mu_{d\downarrow}$ (MeV)	$\mu_{\uparrow}$ (MeV)
0.96	3.0	45.10	21.90	11.10	26.20	−2.19
0.97	2.9	47.70	23.40	11.90	27.90	−2.35
0.98	2.8	50.50	25.10	12.80	29.80	−2.54
0.99	2.7	53.50	26.90	13.80	31.90	−2.74

3.2. Variable Temperature, q and Radius Fixed

In this Subsection, the value of q is set to 0.97, and the quark radius is taken to be 2.5 fm. The dependent variables are the sum of the quarks' momentum, the momentum of the valence quarks, and the violation the GSR. With the q and R chosen, the obtained values for the dependent variables stay within the experimental ranges. Many combinations of values of q and R are posible. The aim here is always to observe the behaviour of the model and not to establish numerical parameters.

Figure 2 shows the dependence of the quarks' momentum (total and valence) with the temperature T, which varies from 31 MeV to 34 MeV. In Table 2, some experimental results of the quarks' mean momentum fraction and the scattering energies Q^2 are given.

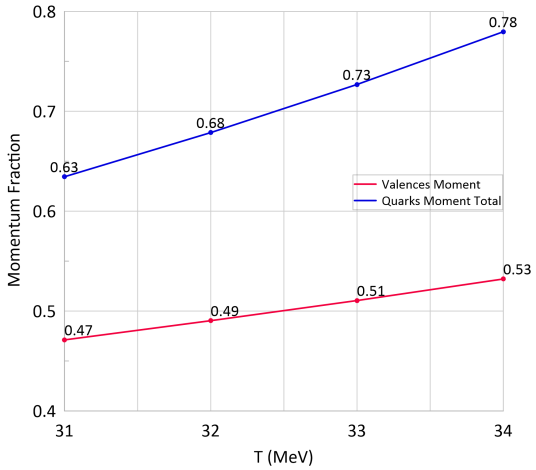

Figure 2. The dependence of quarks' momentum on temperature T in the range 31–34 MeV. The blue line represents the sum of all quarks' momentum. The red line represents the valence quark momentum.

Table 2. The mean momentum, $\langle x \rangle$, carried by quarks ($\langle x \rangle_q$) and gluons ($\langle x \rangle_g$) at different scattering energies, Q^2.

$\langle x \rangle_q$ or $\langle x \rangle_g$	Q^2 (MeV^2)	References
$\langle x \rangle_q = 0.465 \pm 0.023$	15	[2]
$\langle x \rangle_q = 0.3 \pm 0.008$	3.5	[43]
$\langle x \rangle_q = \langle x \rangle_g = 0.50$	10–20	[44]
$\langle x \rangle_g = 0.43 \pm 0.03$	30–100	[45]

Based on Figure 2, one can conclude that the sum of the quarks' momentum increases with the temperature, and that the contribution of the sea quarks increases faster than that

of the valence quarks. Moreover, with a linear extrapolation and considering Table 2, it is possible to relate the temperature and the scattering energy Q^2. The linear approximation in Figure 2 is given by the equation:

$$0.05\,T - 0.92 = \text{total momemtum of quarks} \tag{21}$$

with the determination coefficient $\mathbb{R}^2 = 1$.

Then, based on the linear approach given by Equation (21) and Table 2, it is interesting relate momentum, temperature, and Q^2. Table 3 joins the information about the mean quark's momentum fraction, the scattering energies Q^2, and the temperature that comes from Equation (21).

Table 3. The momentum carried by quarks and gluons with different scattering energies Q^2 and the corresponding temperature, according to Equation (21).

$\langle x\rangle_q$ or $\langle x\rangle_g$	Q^2 (MeV^2)	T (MeV)
$\langle x\rangle_q = 0.465 \pm 0.023$	15	28.3 ± 1.06
$\langle x\rangle_q = 0.3 \pm 0.008$	3.5	24.4 ± 0.16
$\langle x\rangle_q = \langle x\rangle_g = 0.50$	10–20	28.4
$\langle x\rangle_g = 0.43 \pm 0.03$	30–100	29.8 ± 0.6

A relation between the temperature and the transferred momentum is obtained to read:

$$T = 1.8472\ln(Q^2) + 22.491 \tag{22}$$

with the determination coefficient $\mathbb{R}^2 = 0.93$. Figure 3 represents Table 3.

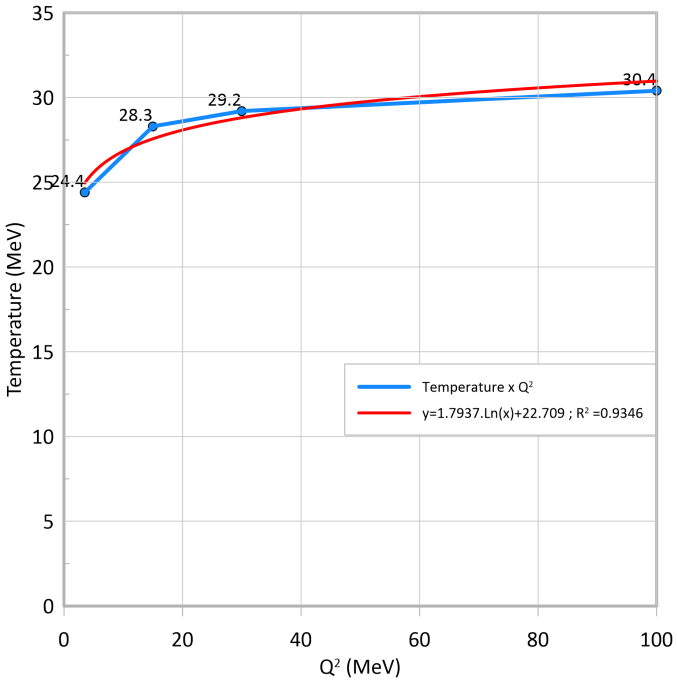

Figure 3. The dependence of the temperature T on Q^2 for $q = 0.97$ and $R = 2.5$ fm.

If the table from [46] is taken into account, with the same relation for temperature and total momentum for the quarks, one has the following linear relation:

$$T = 0.4452\,Q^2 + 18.497 \tag{23}$$

with $\mathbb{R}^2 = 0.9998$. The physical meaning of such an approach is an increase of nucleons' internal energies when there is an inelastic scattering, which causes heating. Some results using relation (23) are shown in Table 4.

Table 4. The momentum carried by quarks and the corresponding temperature, with different Q^2. This table is based on the table from [46] and using Equation (23).

Q^2 MeV^2	$\langle x \rangle_q$	T (MeV)
10	0.22516	22.9032
20	0.45032	27.4064
30	0.67548	31.9096
40	0.90064	36.4128
45	1	38.4

In Figure 4, the violation of the GSR is studied as a function of temperature, $T = 31$–34 MeV. As expected, the difference between the $\bar{D}$ and $\bar{U}$ increases with temperature. The difference grows with temperature is understood as more energy allows more particle to be created, and the Pauli's principle makes the difference to become larger.

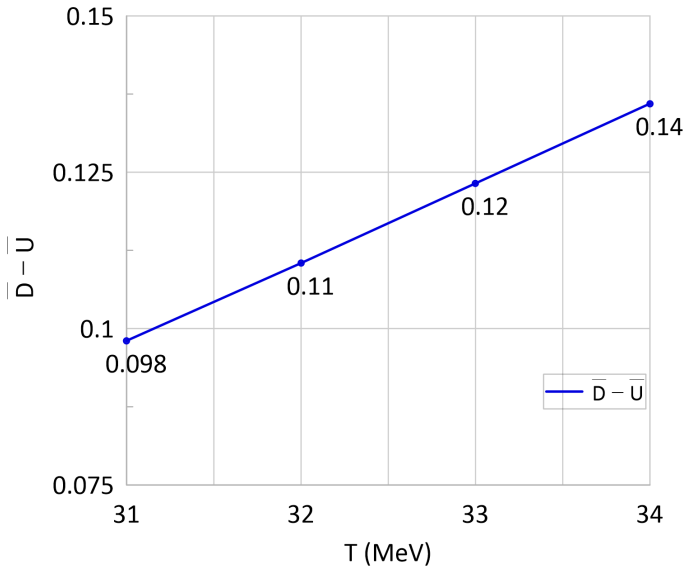

Figure 4. The dependence of the difference $\bar{D} - \bar{U}$ (see Equation (18)) on the temperature T for $q = 0.97$ and $R = 2.5$ fm.

3.3. Variable Radius, q and Temperature Fixed

Here, the value of q is fixed to 0.97, and the temperature is set to 35 MeV. The dependent variables are the sum of momentum and the violation of the GSR. The combination of the values of q and T used keeps quarks momentum to be in the experimentally obtained range.

Figure 5 shows the variation of the sum of the quarks' momentum with the radius. The contribution of valence quarks tends to a constant, while the sea quarks component demonstrates fast increase.

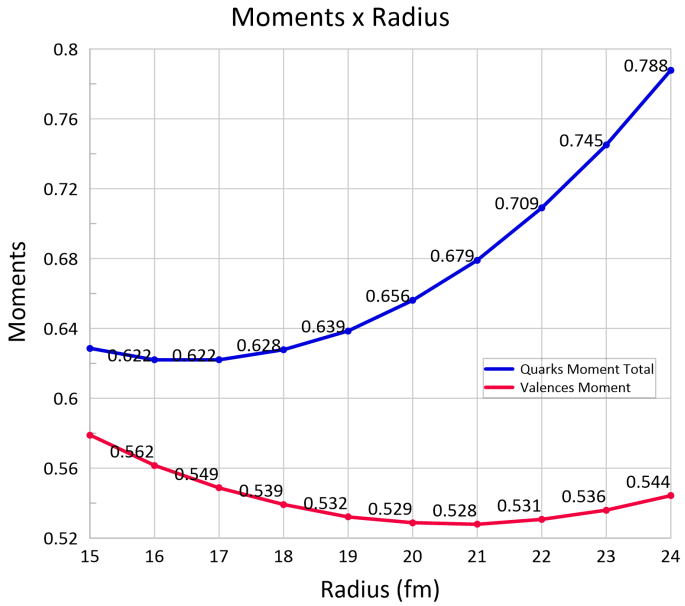

Figure 5. The change of quarks' momentum with the radius, given in fm. The blue line represents the sum for all quarks, and the red line that for the valence quarks only for $q = 0.97$ and $T = 35$ MeV.

From Figure 6, one concludes that the violation of the GSR is related to a large meson cloud.

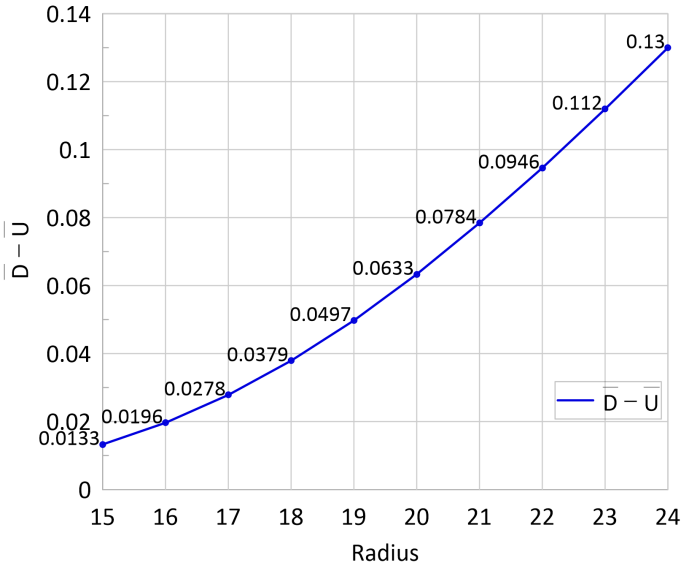

Figure 6. The dependence of $\bar{D} - \bar{U}$ on the radius for $q = 0.97$ and $T = 35$ MeV.

3.4. Variable q, Temperature and Radius Fixed

In this Subsection, the dependence of the momentum of quarks with q is studied. The temperature is kept at 35 MeV, and the radius is set to $R = 2.0$ fm. With these values for T and R, the momentum and the GSR violation lie in the experimentally verified range for a small variation of the q value.

In Figure 7, the quark momentum fraction is shown dependent on the Tsallis variable q. One can observe that with higher non-extensivity, the sum of the quarks' momentum decreases. This indicates that the non-extensivity is related to more gluons, which are self-interacting.

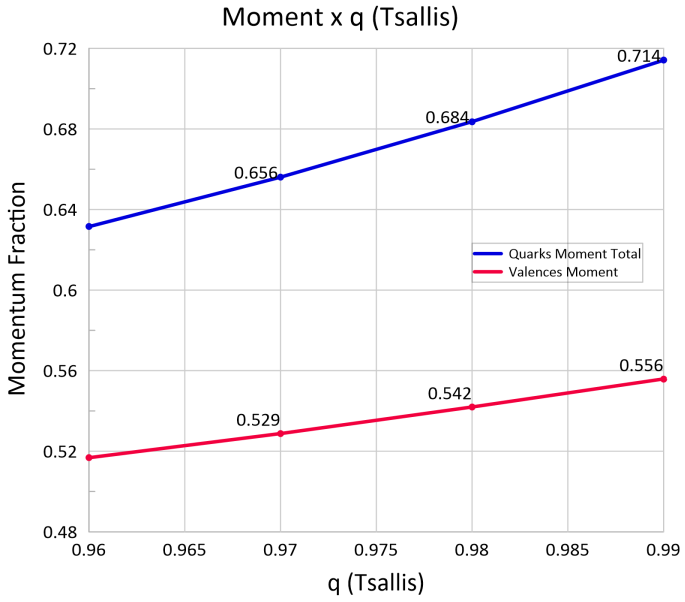

Figure 7. The dependence of the quarks' momentum on q for T = 35 MeV and R = 2.0 fm. The red line represents the sum of the valence quarks, and the blue line includes the sea quarks.

In Figure 8, the difference $\bar{D} - \bar{U}$ is shown depending on the factor q. It increases if the non-extensivity decreases.

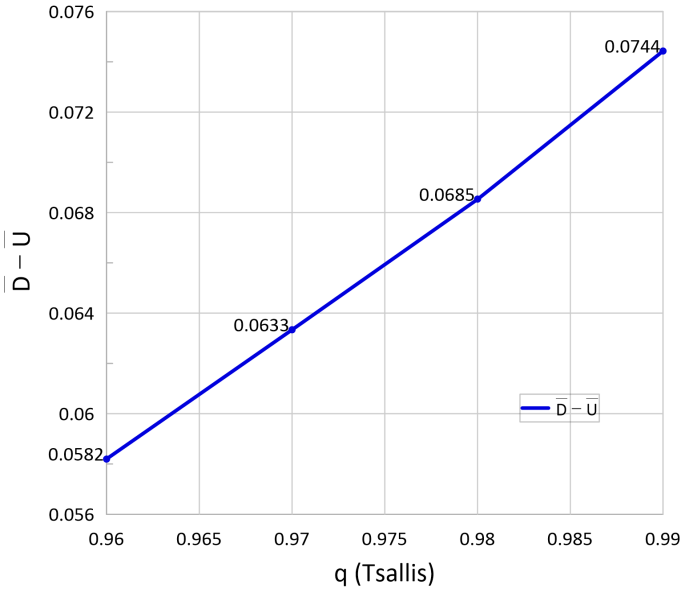

Figure 8. The difference $\bar{D} - \bar{U}$ as a function of q for T = 35 MeV and R = 2.0 fm.

Table 5 shows some values for the radius of gluons and quarks in the model. As predicted, gluons are "larger" than quarks.

Table 5. The radii (R) and momentum sums (M) of gluons (g) and quarks (q) along with the temperature, T, the Tsallis variable, q. The corresponding differences, $\bar{D} - \bar{U}$ (see Equation (18)), are also shown. The gluons momentum is considered of about 46% of the total momentum.

T (MeV)	q	R (fm)	R_q, (fm)	M_g	M_q	$\bar{D} - \bar{U}$
31	0.94	4.58	2.8	0.43	0.57	0.144
32	0.94	4.4	2.6	0.43	0.57	0.122
33	0.94	4.2	2.5	0.43	0.57	0.118

4. Conclusions

In the present paper, studies concerning the variables of the non-extensive statistical model for the nucleon structure function are given. The variations of the nucleon temperature, the radius, and the parameter q of Tsallis statistics are studied. The main objective is to verify that the volume occupied by quarks and gluons may be different. To thsi end, the momentum carried by quarks are invetigated within the existing models.

It is found that not only the radius to be modified but also the temperature, T. The temperature is lower than that obtained in the previous model [23,24] (about 40–60 MeV) to satisfy the sum of the quarks' momentum to be close to the experimental data. In these studies, the quarks' momentum is about 80%. Higher temperatures mean higher energies and more quark-antiquark creation. This increases the total momentum of the quarks. We notice that the same dependence occurs with the scattering energy Q^2 [46]. The linear relationship between T and Q^2 and T and the quarks' total momentum are obtained.

The radius is obtained to be larger (in comparison with previous results [23,24]) to fit the violation of Gottfried's sum rule. The large volume needed to obtain this effect is due to the meson cloud around the valence quarks. Another point to explain is the radius obtained in the present model. Thermodynamical models usually have a radius larger than 1 fm, and some corrections are used. For instance, Bhalerao's study has the finite-size correction, and Mac-Ugaz's [9] paper uses the perturbative correction. The thermodynamic/statistical model with effective confining potential [14,15] also may correct this problem. The initial hypothesis that the gluons gas must occupy a bigger volume than the quarks gas is confirmed.

The q parameter is below 1 in the present model. This result is different from that obtained by [47] or [48]. Those works take measures in the context of quark-gluon plasma, while here, the goal is to obtain the results of the deep inelastic scattering to obtain the structure function. Moreover, the present study is an improvement of an extensive model, which makes the result near 1. It is worth mentioning that there is another approach that obtained $q < 1$ [49] in the context of a bath heath.

To consider the gluon polarization is an interesting point to be studied soon. In this case, the set of Equations (5)–(11) needs to get one more equation to take this into account.

Author Contributions: Conceptualization, L.A.T.; methodology, L.A.T.; software, L.A.T.; validation, L.A.T., C.M. and D.I.d.S.; formal analysis, L.A.T.; investigation, L.A.T.; resources, L.A.T., C.M. and D.I.d.S.; data curation, D.I.d.S.; writing—original draft preparation, C.M.; writing—review and editing, C.M.; visualization, D.I.d.S. All authors have read and agreed to the published version of the manuscript.

Funding: This research received no external funding.

Data Availability Statement: Not applicable.

Acknowledgments: L.A.Trevisan thanks Airton Deppman for the invitation to participate in this Special Issue.

Conflicts of Interest: The authors declare no conflict of interest.

References

1. Halzen, F.; Martin, A.D. *Quarks and Leptons: An Introductory Course in Modern Particle Physics*; John Wiley and Sons: Singapore, 1980; p. 203.
2. Sloan, T.; Smadja, G.; Voss, R. The quark structure of the nucleon from the cern muon experiments. *Phys. Rep.* **1988**, *162*, 46. [CrossRef]
3. Alexandrou, C.; Constantinou, M.; Hadjiyiannakou, K.; Jansen, K.; Panagopoulos, H.; Wiese, C. Gluon momentum fraction of the nucleon from lattice QCD. *Phys. Rev. D* **2017**, 054503. [CrossRef]
4. Xiangdong, J.; Tang, J.; Hoodbhoy, P. The spin structure of the nucleon in the ssymptotic limit. *Phys. Rev. Lett.* **1996**, *76*, 740. [CrossRef]
5. Chen, X.-S.; Sun, W.-M.; Lü, X.-F.; Wang, F.; Goldman, T. Do gluons carry half of the nucleon momentum? *Phys. Rev. Lett.* **2009**, *103*, 062001. 103.062001 [CrossRef]

6. Angelini, C.; Pazzi, R. Thermodynamical information on quark matter from the nucleon valence quark distribution. *Phys. Lett.* **1982**, *113B*, 343. [CrossRef]
7. Angelini, C.; Pazzi, R. On the scaling violations of a thermodynamical valence quark distribution. *Phys. Lett.* **1984**, *135B*, 473. [CrossRef]
8. Cleymans, J.; Thews, R.L. Statistical model for the structure functions of the nucleon. *Z. Phys. C* **1988**, *37*, 315. [CrossRef]
9. Mac, E.; Ugaz, E. A statistical model of structure functions and quantum chromodynamics. *Z. Phys. C* **1989**, *43*, 655. [CrossRef]
10. Mirez, C.; Tomio, L.; Trevisan, L.A.; Frederico, T. Quark sea asymmetry of the nucleon. *Nucl. Phys. B (Proc. Suppl.)* **2010**, *199*, 252–257. [CrossRef]
11. Mirez, C.; Tomio, L.; Trevisan, L.A.; Frederico, T. Statistical Quark model for the nucleon structure function. *AIP Conf. Proc.* **2009**, *1139*, 202. [CrossRef]
12. Mirez, C.; Tomio, L.; Trevisan, L.A.; Frederico, T. Improved statistical QCD model for the quark content of the nucleon. *Int. J. Modern. Phys. D* **2010**, *19*, 1697–1701. [CrossRef]
13. Mirez, C. Improved statistical quark model for the nucleon structure function. *AIP Conf. Proc.* **2010**, *1245*, 137–140. [CrossRef]
14. Trevisan, L.A.; Tomio, L.; Frederico, T. Strangeness content and structure function of the nucleon in a statistical quark model. *Eur. Phys. J. C* **1999**, *11*, 351. [CrossRef]
15. Trevisan, L.A.; Frederico, T.; Mirez, C. Nucleon flavor asymmetry in a statistical quark model. *Nucl. Phys. A* **2007**, *790*, 522c–525c. [CrossRef]
16. Trevisan, L.A.; Mirez, C.; Tomio, L.; Frederico, T. Quark sea structure functions of the nucleon in a statistical model. *Eur. Phys. J. C* **2008**, *56*, 211. [CrossRef]
17. Bickerstaff, R.P.; Londergan, J.T. Proton and neutron structure functions in a Fermi-gas approximation. *Phys. Rev. D* **1990**, *42*, 3621. [CrossRef]
18. Devanathan, V.; Karthiyayini, S.K. A Thermodynamical bag model for nucleon structure functions. *Mod. Phys. Lett. A* **1991**, *9*, 3455. [CrossRef]
19. Devanathan, V.; McCarthy, J.S. A Thermodynamical bag model for the nucleon spin. *Mod. Phys. Lett. A* **1996**, *11*, 147. [CrossRef]
20. Bhalerao, R.S. Statistical model for the nucleon structure functions. *Phys. Lett. B* **1996**, *380*, 1. [CrossRef]
21. Chodos, A.; Jaffe, R.L.; Johnson, K.; Thorn, C.B.; Weisskopf, V.F. New extended model of hadrons. *Phys. Rev. D* **1974**, *9*, 3471. [CrossRef]
22. Jaffe, R.L. Deep-inelastic structure functions in an approximation to the bag theory. *Phys. Rev. D* **1975**, *11*, 1953. [CrossRef]
23. Trevisan, L.A. The polarized structure function from the nonextensive statistics. *Int. J. Mod. Phys. E* **2016**, *25*, 165010. [CrossRef]
24. Trevisan, L.A.; Mirez, C. A Nonextensive statistical model for the nucleon structure function. *Int. J. Mod. Phys. E* **2013**, *22*, 1350044. [CrossRef]
25. Towell, R.S.; et al. [E866 Collaboration]. Improved measurement of the $\bar{d}/\bar{u}$ asymmetry in the nucleon sea. *Phys. Rev. D* **2001**, *64*, 052002. [CrossRef]
26. Tsallis, C. Possible generalization of Boltzmann-Gibbs statistics. *J. Stat. Phys.* **1988**, *52*, 479. [CrossRef]
27. Curado, E.M.F.; Tsallis, C. Generalized statistical mechanics: Connection with thermodynamics. *J. Phys. A* **1991**, *24*, L69–L72. [CrossRef]
28. Bhalerao, R.; Kelkar, N.; Ram, B. Model for polarized and unpolarized parton density functions in the nucleon. *Phys. Lett. B* **2000**, *476*, 285. [CrossRef]
29. Hwa, R.C. Evidence for valence-quark clusters in nucleon structure functions. *Phys. Rev. D* **1980**, *22*, 759. [CrossRef]
30. Hwa, R.C. Clustering and hadronization of quarks: A treatment of the low-p_T problem. *Phys. Rev. D* **1980**, *22*, 1593. [CrossRef]
31. Deppman, A. Thermodynamics with fractal structure, Tsallis statistics, and hadrons. *Phys. Rev. D* **2016**, *93*, 054001. [CrossRef]
32. Cardoso, P.H.G.; da Silva, T.N.; Deppman, A.; Menezes, D.P. Quark matter revisited with non-extensive MIT bag model. *Eur. Phys. J. A* **2017**, *53*, 191. [CrossRef]
33. Cottingham, W.N.; Greenwood, D.A. *An Introduction to the Standard Model of Particle Physics*; Cambridge University Press: Cambridge, UK, 2007.
34. Parvan, A.S.; Bhattacharyya, T. Hadron transverse momentum distributions of the Tsallis normalized and unnormalized statistics *Eur. Phys. J. A* **2020**, *56*. [CrossRef]
35. Anthony, P.L.; et al. [E142 Collaboration]. Deep inelastic scattering of polarized electrons by polarized 3He and the study of the neutron spin structure. *Phys. Rev. D* **1996**, *54*, 6620. [CrossRef] [PubMed]
36. Abe, K.; et al. [E143 Collaboration]. Measurements of the proton and deuteron spin structure functions g_1 and g_2. *Phys. Rev. D* **1998**, *58*, 112003. [CrossRef]
37. Abe, K.; et al. [E154 Collaboration]. Next-to-leading order QCD analysis of polarized deep inelastic scattering data. *Phys. Lett. B* **1997**, *405*, 180. [CrossRef]
38. Abe, K.; et al. [E154 Collaboration]. Precision Determination of the Neutron Spin Structure Function g_1^n. *Phys. Rev. Lett.* **1997**, *79*, 26. [CrossRef]
39. Adeva, B.; et al. [Spin Muon Collaboration]. Next-to-leading order QCD analysis of the spin structure function g_1. *Phys. Rev. D* **1998**, *58*, 112002. [CrossRef]
40. Ackerstaff, K.; et al. [Hermes Collaboration]. Measurement of the neutron spin structure function g_1^n with a polarized ^{3}He internal target. *Phys. Lett. B* **1997**, *404*, 383. [CrossRef]

41. Peng, J.C. Flavor asymmetry of the nucleon sea. *Nucl. Phys. A* **2001**, *684*, 80–88. [CrossRef]
42. Peng, J.C.; et al. [FNAL E866/NuSea Collaboration]. $\bar{d}/\bar{u}$ asymmetry and the origin of the nucleon sea. *Phys. Rev. D* **1998**, *58*, 092004. [CrossRef]
43. Politzer, H.D. μ-p scattering and the glue fraction of the proton. *Nucl. Phys.* **1977**, *B122*, 237. [CrossRef]
44. Abramowicz, H.; de Groot, J.G.H.; Knobloch, J.; May, J.; Palazzi, P.; Para, A.; Ranjard, F.; Savoy-Navarro, A.; Schlatter, D.; Steinberger, J.; et al. Neutrino and antineutrino charged-current inclusive scattering in iron in the energy range $20 < E_v < 300$ GeV. *Z. Phys.* **1983**, *C17*, 283. [CrossRef]
45. De Groot, J.G.H.; Hansl, T.; Holder, M.; Knobloch, J.; May, J.; Paar, H.P.; Palazzi, P.; Para, A.; Ranjard, F.; Schlatter, D.; et al. Inclusive interactions of high-energy neutrinos and antineutrinos in iron. *Z. Phys.* **1979**, *C1*, 143. [CrossRef]
46. Jahan, A.; Choudhury, D.K. Momentum fractions of quarks and gluons in a self-similarity based model of proton. *Mod. Phys. Lett.* **2012**, *A27*, 1250193. [CrossRef]
47. Teweldeberhan, A.M.; Miller, H.G.; Tegen, R. Generalized statistics and the formation of a quark-gluon plasma. *Int. J. Mod. Phys. E* **2012**. [CrossRef]
48. Teweldeberhan, A.M.; Miller, H.G.; Tegen, R. Kappa deformed statistics and the formation of a quark gluon plasma. *Int. J. Mod. Phys. E* **2003**. [CrossRef]
49. Biró, T.S.; Barnafoldi, G.G.; Ván, P. Quark-gluon plasma connected to finite heat bath. *Eur. Phys. J. A* **2013**, *49*, 110. [CrossRef]